THE ASTROPHYSICAL JOURNAL, 339:729–741, 1989 April 15

KINEMATICS AND IONIZATION OF EXTENDED GAS IN ACTIVE GALAXIES. V. THE SEYFERT GALAXY NGC 5548

A. S. WILSON[1]
Astronomy Program, University of Maryland
XUENING WU AND T. M. HECKMAN[2,3]
Astronomy Program, University of Maryland
J. A. BALDWIN
Department of Astronomy, Ohio State University
AND
B. BALICK[2]
Astronomy Department, University of Washington
Received 1988 March 29; accepted 1988 August 29

ABSTRACT

We report a detailed optical investigation of the circumnuclear region of the Seyfert galaxy NGC 5548. The new observational material comprises a deep photographic plate, direct images of the inner regions in both continuum and emission lines, and medium- to high-dispersion long-slit spectroscopy covering the spectral regions 4200–5350 Å and 6250–7000 Å.

An emission-line nebulosity, of extent 12″ × 8″ (4.0 × 2.7 kpc) at 0.5% of the central peak intensity, surrounds the nucleus (the peak of both line and continuum light). The inner isophotes of the [O III] λ5007 image align with the 13″ (4.4 kpc) scale triple radio source, as is commonly the case in Seyfert galaxies with such radio structure. The morphology in Hα + [N II] λλ6548, 6584 is quite different, showing an extended region of low-excitation gas to the northeast of the nucleus. The profiles of narrow Hβ and [O III] λ5007 right at the nucleus are also different, with the former line showing a double-peaked structure. Spatial maps of line profiles show that Hβ is narrower than [O III] λ5007 over the whole nebulosity. The velocity field of much of the gas is dominated by rotational motions, with the nucleus being blueshifted with respect to the systemic velocity derived from the rotation curve. Both the kinematic center of the rotation curve and the location of the broadest [O III] λ5007 lines appear to be displaced from the nucleus. The flux ratio [O III] λ5007/Hβ decreases from $\simeq 10$ at the nucleus to $\simeq 0.6$–4 in the northeastern nebulosity where both lines are narrow.

The relative strengths of Hβ, [O III] λ5007, Hα, [N II] λ6584, [S II] λλ6717, 6731, and [O I] λ6300 in the extended nebulosity to the northeast are consistent with two gaseous components projected on top of each other along our lines of sight. One component emits high-excitation, broad lines and is presumably ionized by the Seyfert nucleus, while the other is of low excitation, radiates narrow lines, and appears to originate in H II regions ionized by hot stars. The bolometric luminosity of the hot stars is of order 10^8–10^9 $L_\odot$.

Subject headings: galaxies: individual (NGC 5548) — galaxies: internal motions — galaxies: nuclei — galaxies: Seyfert

I. INTRODUCTION

NGC 5548 has long been known to be a Seyfert galaxy (e.g., Burbidge 1970), and the nucleus has been extensively studied. Intercomparison of the large number of published optical spectra (Anderson 1970, 1971; de Bruyn and Sargent 1978; de Bruyn 1980; Peterson *et al.* 1982; Wilson and Ulvestad 1982; Malkan and Filippenko 1983; Osterbrock 1984; de Robertis 1985; Crenshaw and Peterson 1986; Chuvaev 1987; Peterson 1987; Stirpe, de Bruyn, and van Groningen 1987) shows clear evidence for variability of the intensities and profiles of the broad emission lines and of the continuum luminosity. Recent interpretations of the variations of the Balmer lines have favored a double- or multicomponent broad-line region (Peterson 1987; Stirpe, de Bruyn, and van Groningen 1987), possibly a supermassive binary, with each binary component having its own broad-line region (Peterson, Korista, and Cota 1987). Analogous investigations have been made with the *IUE* of the structures and variability of the ultraviolet emission lines and continuum (Barr, Willis, and Wilson 1983; Ulrich and Boisson 1983; Wamsteker *et al.* 1984). Ground-based photometric observations at infrared wavelengths have been published by a number of workers (e.g., Rieke 1978; McAlary, McLaren, and Crabtree 1979), and the galaxy has been included in a number of investigations of the far-infrared emission of active galaxies using *IRAS* data (e.g., Ward *et al.* 1987). NGC 5548 is a bright X-ray source (Elvis *et al.* 1978; Tananbaum *et al.* 1979) with a hard spectrum typical of type 1 Seyferts (Hayes *et al.* 1980; Mushotzky *et al.* 1980). In the radio band, the galaxy shows a compact nuclear source straddled by two lobes with total source extent 13″ (Wilson and Ulvestad 1982).

The present paper is a continuation of our program investigating the properties of spatially extended ionized gas in nearby active galaxies. Extended emission lines were found in

[1] Visiting Astronomer, Cerro Tololo Inter-American Observatory, which is operated by the Association of Universities for Research in Astronomy, Inc., under contract with the National Science Foundation.
[2] Visiting Astronomer, Kitt Peak National Observatory, which is operated by the Association of Universities for Research in Astronomy, Inc., under contract with the National Science Foundation.
[3] Alfred P. Sloan Foundation Fellow.

NGC 5548 by Wilson and Ulvestad (1982), but their spatial resolution and coverage, spectral resolution, and sensitivity were inadequate for a detailed investigation. Here we present a deep continuum plate, direct images of the central region in emission lines and continua, and long-slit spectroscopy in the green and the red. In particular, the long-slit observations of Hβ and [O III] λ5007 fully cover the ionized nebulosity revealed by the direct images, allowing maps of the gaseous kinematics and excitation, sampled on the scale of the seeing, to be obtained.

In § II we describe the observations and their reduction. Section III presents the results on the gaseous morphology, line profiles, velocity field, and line fluxes and flux ratios. In § IV we discuss the composite nature of the gaseous nebulosity in NGC 5548, and in § V we summarize our conclusions. A Hubble constant of 75 km s^{-1} Mpc^{-1} is used throughout the paper.

II. OBSERVATIONS AND REDUCTIONS

a) Direct Imaging

NGC 5548 was observed on 1980 March 16, with an intensified SIT Vidicon system (the "video camera") using the 4 m telescope at the Kitt Peak National Observatory (KPNO) as part of a survey of the morphology of emission-line gas and starlight in Seyfert galaxies. Images were obtained through a standard V filter and through narrow-band ($\Delta\lambda/\lambda \sim 1\%$) interference filters centered in wavelength on the redshifted [O III] λ5007 line, on the Hα + [N II] $\lambda\lambda$6548, 6584 lines ("on" images), and on the appropriate adjacent continuum ("off" images). After processing these images (flat-fielding and geometric rectification) using standard KPNO software, the images were all coaligned and the "on" and "off" images were differenced to yield continuum-free images of the [O III] and Hα + [N II] emitting gas. The final images are 256 × 256 pixels in size with a pixel size of 0".29.

b) Long-Slit Spectroscopy

The first long-slit spectroscopic observations were obtained with SIT Vidicon detectors on the Ritchey-Chrétien (R-C) spectrograph of the Cerro Tololo Inter-American Observatory (CTIO) 4.0 m telescope. A 16 mm Vidicon was used on the four nights 1982 March 31/April 1 to April 3/4, and a 40 mm Vidicon on the single night 1984 March 22/23. The slit position coverage obtained is illustrated in Figure 1. Seventy spatial increments (i.e., along the slit) and either 830 (1982 observations) or 1650 (1984 observations) spectral channels (i.e., along the dispersion direction) were used. In 1982 (1984) each spatial increment corresponded to 0".55 (1".2), giving a useful slit length of 38" (84"). Seeing ranged between 1" and 3", corresponding to net resolutions along the slit of 1".7–3".5 (FWHM). The slit width was 1".5 for all observations of NGC 5548, but was increased to 6".6 for observations of flux standard stars. With the narrower slit, the spectral resolution was 1.6 Å (FWHM) or 0.55 Å (1 σ) for the 1982 data, and 2.2 Å (FWHM) or 0.9 Å (1 σ) for the 1984 data. Spectral coverage was $\simeq$490 Å in 1982, including Hβ and [O III] $\lambda\lambda$4959, 5007, and was 1150 Å in 1984, including Hβ, Hγ, and [O III] $\lambda\lambda$4363, 4959, 5007. In view of the weakness of Hγ and [O III] λ4363 off the nucleus, our kinematic analysis is restricted to Hβ and [O III] λ5007. Other aspects of the observing and reduction procedures followed closely the description of Wilson, Baldwin, and Ulvestad (1985, hereafter Paper I).

The off-nuclear emission lines in NGC 5548 are weak, and errors in the recession velocities are dominated by signal-to-noise considerations. A comparison was made between the velocities derived from the 1982 and 1984 data at nine common positions in the nebulosity. For the 18 measurements of peak and mean velocity (the latter obtained from the mean wavelength $\sum_\lambda F_\lambda \lambda / \sum_\lambda F_\lambda$, where F_λ is the continuum-subtracted line flux), the rms deviation about the relation $V_{1982} = V_{1984}$ is 29 km s^{-1}, and the mean deviation is 3 km s^{-1}.

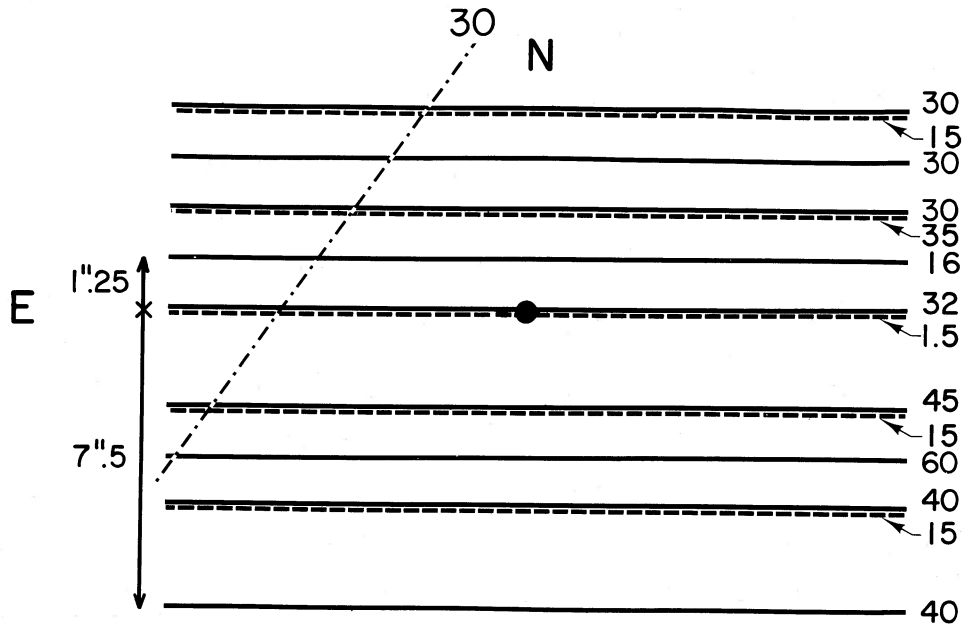

FIG. 1.—Illustration of slit positions obtained in observations of NGC 5548. The solid lines refer to the CTIO observations covering 4760–5250 Å (1982), the dashed ones to the CTIO observations covering 4200–5350 Å (1984), and the dot-dash one to the KPNO observation covering 6250–7000 Å (1987). The filled circle represents the optical nucleus (i.e., brightest point on acquisition TV). The lengths of the lines are arbitrary; the total slit length was 38" in 1982, 84" in 1984, and $\simeq$4' in 1987. The numbers at one end of each line give the total integration time (in minutes) obtained at that slit position over the different observing nights.

In order to perform a more extensive investigation of the ionization state of gas to the northeast of the nucleus of NGC 5548, an additional long-slit observation was obtained with the KPNO 4 m telescope on 1987 April 27. The slit was aligned in p.a. 144° and displaced 6″ east of the Seyfert nucleus (Fig. 1). The detector was the TI No. 3 CCD chip mounted on the R-C spectrograph, and the spectral coverage was 6250–7000 Å. With 2 × 2 pixel binning on the chip, the pixel sizes were 0″.89 along the slit and 1.9 Å along the dispersion direction. Including the effects of seeing and slit width (2″), the spatial resolution along the slit and the spectral resolution were $\simeq 2''$ and 3.8 Å (both FWHM), respectively, the latter corresponding to 170 km s^{-1} at Hα.

III. RESULTS

a) *Morphological Characteristics*

A description of the morphology of NGC 5548 has been published by Adams (1977). He notes the amorphous nuclear bulge (diameter 18″ = 6 kpc), from which two inner spiral arms, or an inner ring (dimensions 27″ × 33″ = 9 × 11 kpc), emerge. Outside this there is a diffuse ring or system of nearly circular spiral arms with dimensions 50″ × 57″ = 17 × 19 kpc. Finally there is an extremely faint outer ring or halo approximately 2′ = 42 kpc in diameter. All these features may be seen in a deep 48 inch (1.2 m) Palomar Schmidt plate taken by A. G. de Bruyn, and reproduced here as Figure 2 (Plate 8). NGC 5548 has been classified as (R′)SA(s)0/a (de Vaucouleurs, de Vaucouleurs, and Corwin 1976) and (R′)SA(r)0/a (Simkin, Su, and Schwarz 1980). Su and Simkin (1980) describe it as a DR galaxy, containing both an inner disk and outer rings.

Figure 3 shows two continuum images and the continuum-subtracted [O III] λ5007 and Hα + [N II] λλ6548, 6584 images of the central regions of NGC 5548 from the video camera observations. The beginning of the inner spiral arm or ring may be seen some 17″ (5.7 kpc) to the southwest of the nucleus on the *V*-band image.

[O III] λ5007 shows a smooth distribution of light with peak coincident with that of the adjacent continuum to 0″.2. The brightest isophotes are elongated in p.a. $\simeq 162°$, which is very close to the axis of the 13″ (4.4 kpc) size triple nuclear radio

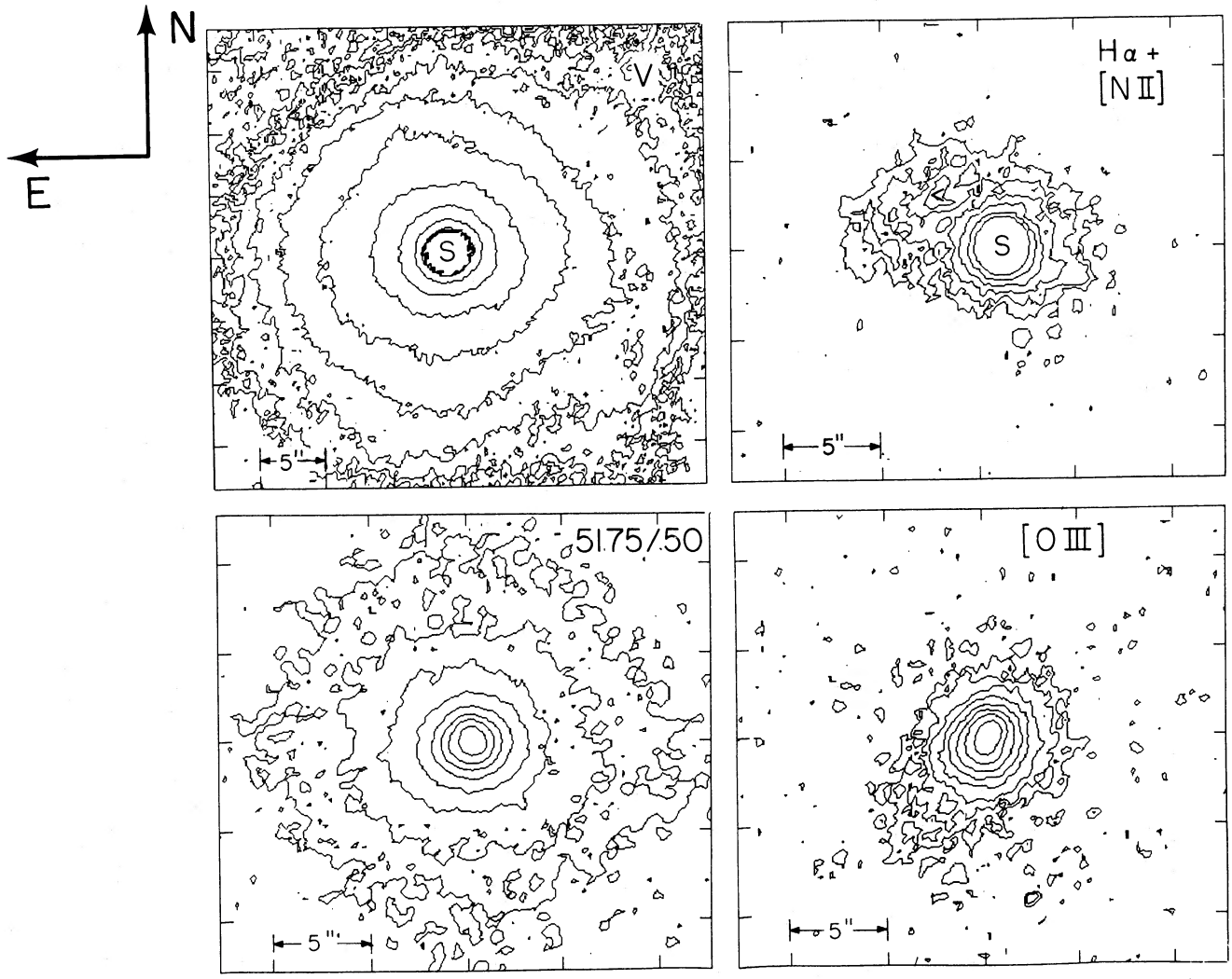

FIG. 3.—Direct images of NGC 5548 obtained with the "video camera" on the KPNO 4 m telescope. The *V* band (*top left*) and Hα + [N II] (*top right*) images are saturated in the center, as indicated by the letter *S*. The continuum image through a filter centered on 5175 Å, with passband 50 Å (*bottom left*), and the [O III] λ5007 image (*bottom right*) are not saturated. The symbol "<" indicates a local minimum in the Hα + [N II] map. Contours are drawn at intervals of a factor of 2 in brightness.

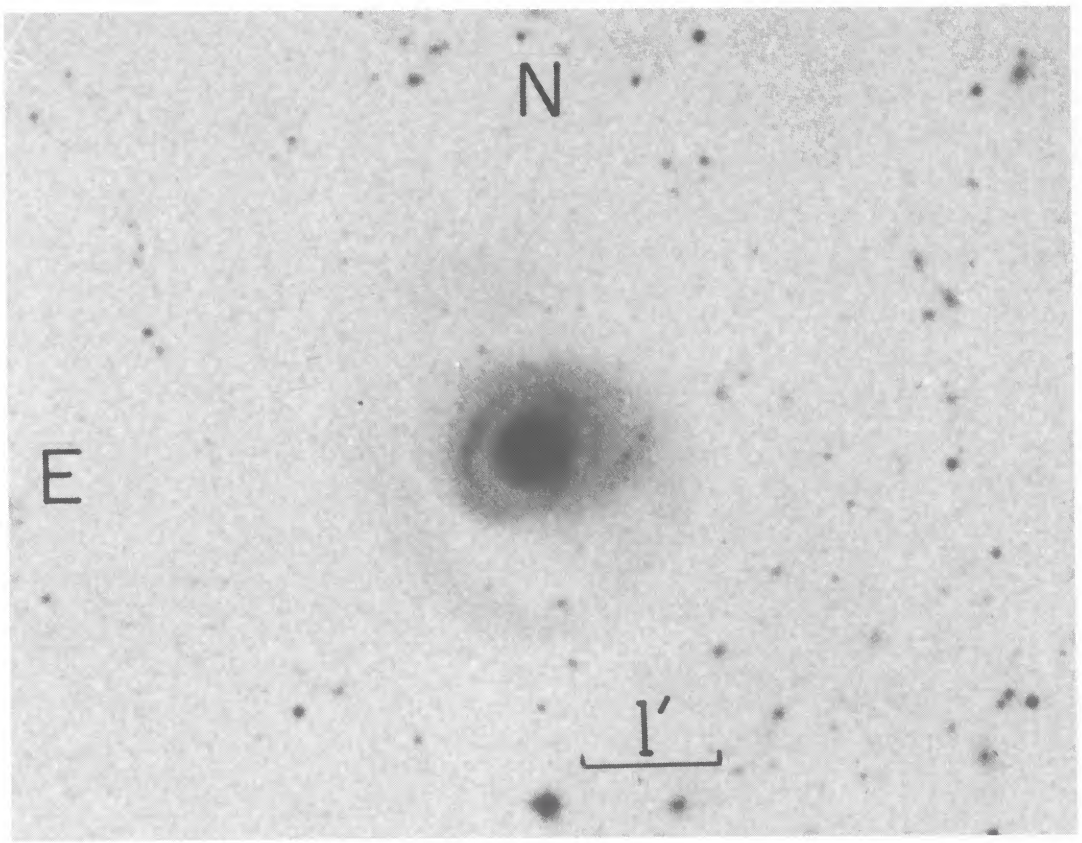

FIG. 2.—Direct plate of NGC 5548 obtained by A. G. de Bruyn with the Palomar 48 inch (1.2 m) Schmidt telescope on 1977 April 20/21. The exposure time was 75 minutes on a IIIa-J plate through a WR2C filter.

WILSON *et al.* (*see* **339**, 731)

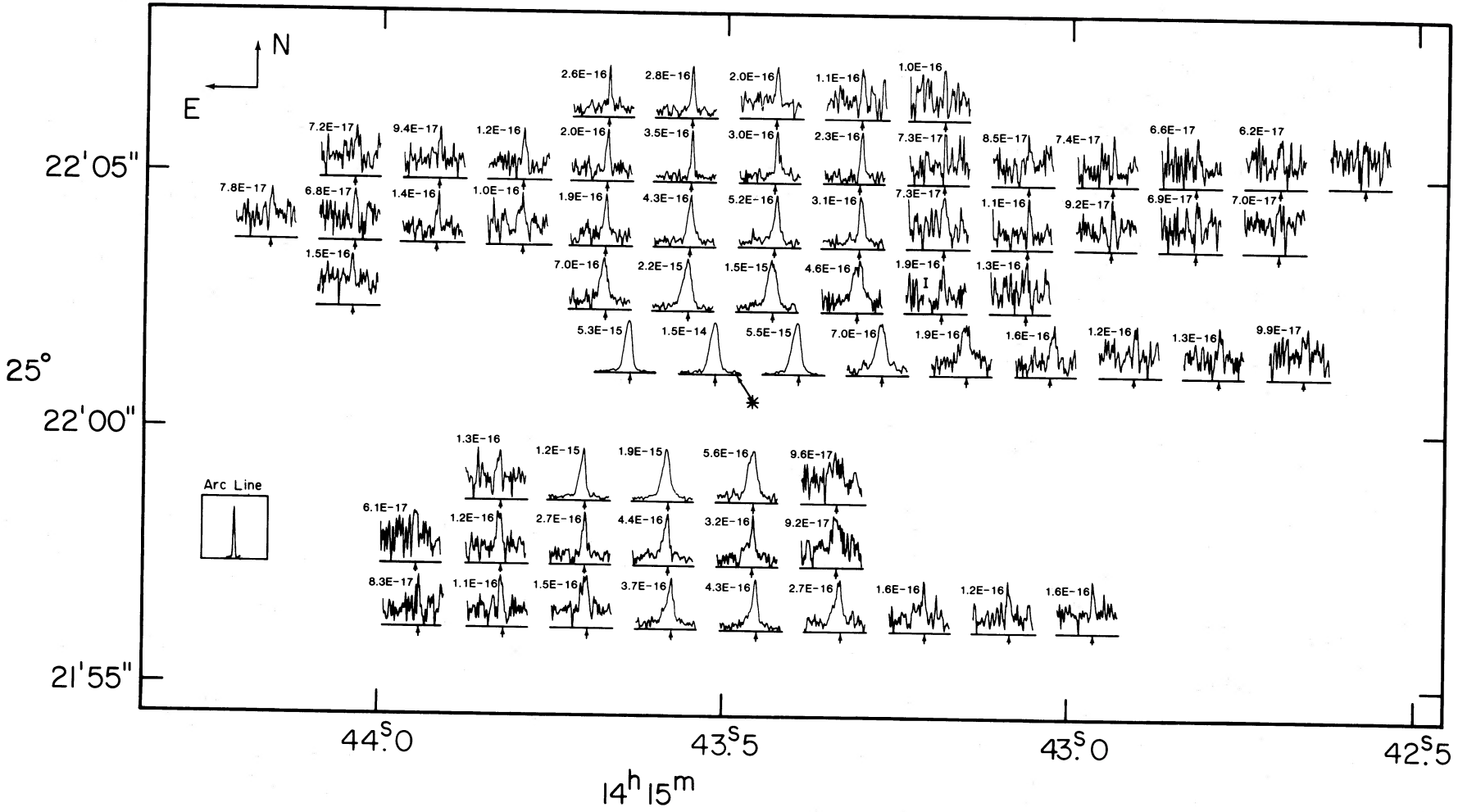

FIG. 4*a*

FIG. 4.—(*a*) Profiles of [O III] λ5007 in NGC 5548. Each profile is normalized so that the difference between the maximum and minimum monochromatic fluxes over the range of wavelength plotted is the same physical height. For each profile, the vertical arrow indicates 5133 km s^{-1}, the heliocentric systemic velocity (§ III*c*), and the total range of velocity plotted is 3030 km s^{-1}. The number next to each profile gives an estimate of the peak monochromatic flux in the line (in ergs cm^{-2} s^{-1} $Å^{-1}$) after subtraction of the continuum. The locations of ion events, which have been removed, are indicated by the letter *I*. The distance between adjacent profiles in the vertical direction is usually 1".25, and in the horizontal it is 1".65. The profiles and listed peak monochromatic fluxes refer to an area of 1".5 × 1".65 (vertically × horizontally), centered at the tip of the arrow. The arc line shows the instrument resolution. The nominal position of the nucleus is indicated by the asterisk. Note that the profile closest to the nucleus is actually [O III] λ4959 ([O III] λ5007 was saturated at this position), but the peak monochromatic flux given is appropriate to [O III] λ5007. Right ascension and declination scales have been added using the accurate nuclear position determined by Clements (1981). However, the profiles may actually be displaced by up to 0".5 from their nominal positions because of differential atmospheric refraction (see text). (*b*) Profiles of Hβ in NGC 5548; other details as for (*a*). In particular, the velocity at the arrow and the range of velocities plotted are the same as in (*a*).

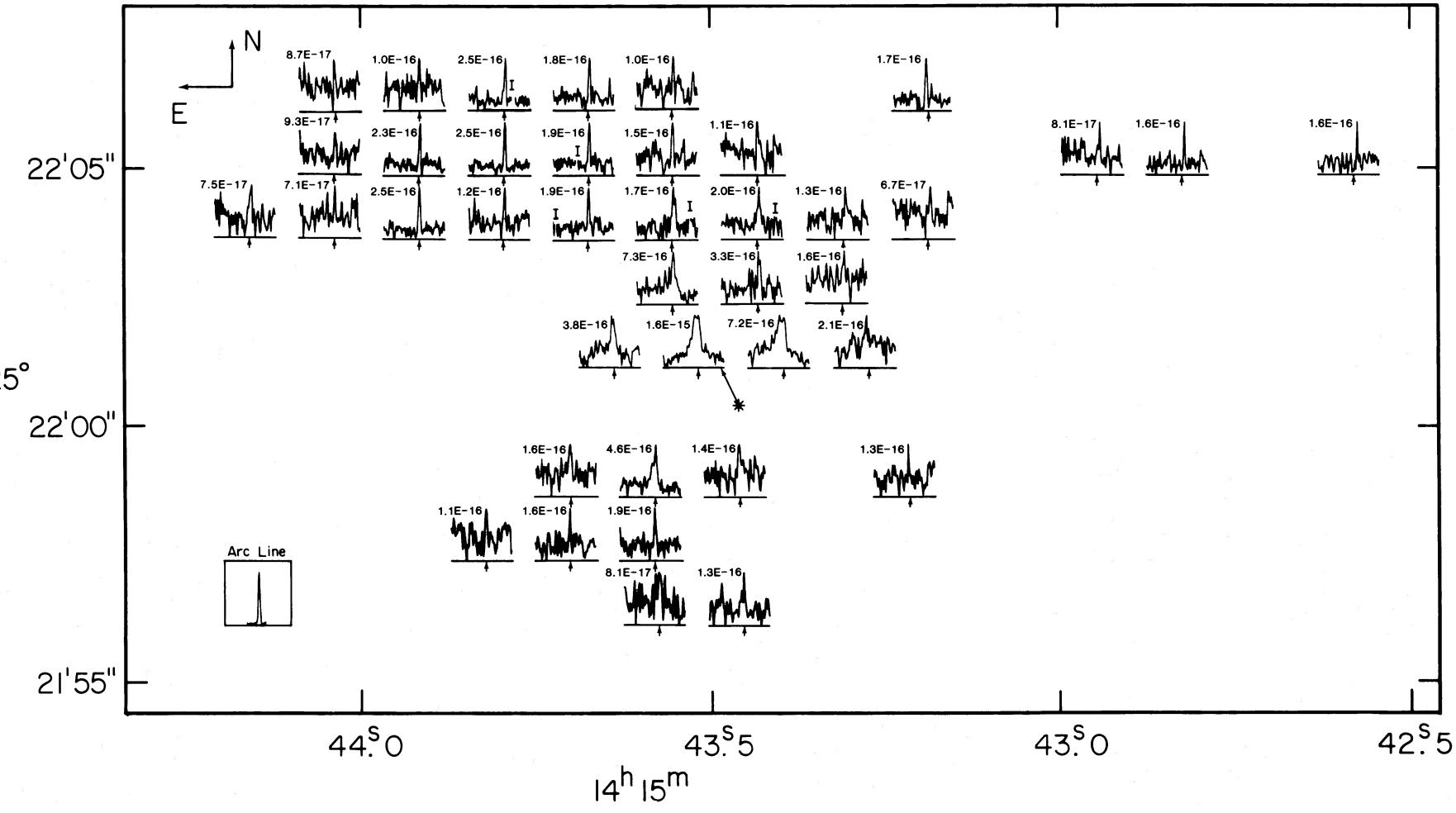

FIG. 4*b*

source (p.a. $\simeq 160°$; Wilson and Ulvestad 1982). At fainter levels, the [O III] major-axis position angle decreases to $\simeq 140°$, which is closer to the elongation of the nuclear bulge and inner ring/spiral arms (p.a. 125°–130°, Fig. 2). The nature of these relationships is discussed in § IV*b*. The overall extent of the detected [O III] light is 12″ × 8″ (4.0 × 2.7 kpc), with the faintest isophote representing ~0.5% of the peak.

The Hα + [N II] λλ6548, 6584 image is saturated in the center, so no useful information may be obtained within ≈1″ of the nucleus. At fainter levels, the image is quite different from that of [O III]. There is a protrusion beginning about 3″ southwest of the nucleus and extending westward. This feature is weakly present in the [O III] picture. Faint, diffuse Hα + [N II] emission is seen to the northeast; this outer nebulosity is also apparent in the Hβ map obtained from the long-slit spectroscopy (Fig. 4*b*). The overall diameter of the Hα + [N II] light at the faintest level (~0.5% of the peak) is 13″ × 8″ (4.4 × 2.7 kpc).

b) Line Profiles and Widths

Figures 4*a* and 4*b* give the distributions of the line profiles of [O III] λ5007 and Hβ. These diagrams were obtained from the 1982 data, after binning together 3 pixels along the slit. It should be emphasized that no attempt was made to maintain a uniform sensitivity for spectra obtained at different locations. In particular, the exposure times tended to be shorter for slit positions close to the nucleus than for those farther out (Fig. 1), so the outline of the region covered by profiles largely reflects this sensitivity variation rather than the true shape of the nebulosity. Also, because NGC 5548 was observed from CTIO at significant air mass (1.75–2.0), differential atmospheric refraction between the effective wavelength of the acquisition TV and the spectral region studied may result in small shifts (<0.″5) of the profiles relative to their nominal locations.

Examination of the [O III] λ5007 distribution (Fig. 4*a*) shows that the peak line flux drops by a factor of ~200 from the nucleus to the edge of the nebulosity, in agreement with the direct imaging (note that only extremely weak line emission was found in the spectrum obtained with the slit displaced 7.″5 south of the nucleus and is not included in Fig. 4). Near the nucleus the lines change their profiles on the scale of the seeing, so the exact profile at any location is obviously sensitive to slit size and centering. The nuclear [O III] profile shows a blueward slanting asymmetry, as already noted for NGC 5548 by Heckman *et al.* (1981) and Whittle (1985).

The Hβ map (Fig. 4*b*) contains fewer profiles because the line is generally weaker than [O III] λ5007. The spectral region plotted is not sufficient to cover the *very* broad Hβ emission (from the broad-line region), which shows up as a curved baseline to the profiles close to the nucleus. The narrow-line component of Hβ right at the nucleus is double-peaked or at least flat-topped (Fig. 5), with the separation in velocity of the two Hβ peaks being 180 km s^{-1}. Several of our independent spectra through the nucleus, as well as the ones published by Heckman *et al.* (1981) and de Robertis (1985), confirm this difference between the nuclear Hβ profile and the more sharply peaked [O III] emission. The velocity of the peak of nuclear [O III] emission lies in between those of the two Hβ peaks. The double-peaked nuclear Hβ profile may reflect integration over a steep, nuclear velocity gradient and is reminiscent of the profiles expected from a tilted rotating disk or a bipolar outflow. Another striking feature of Figure 4*b* is the extreme narrowness of the off-nuclear Hβ profiles, especially in the northeast quadrant. The off-nuclear Hβ emission is always narrower than [O III] λ5007 and is often unresolved or only marginally resolved in velocity with our 97 km s^{-1} resolution (FWHM).

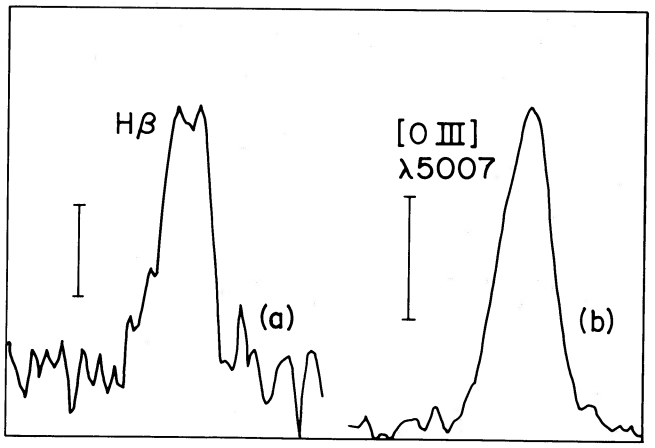

FIG. 5.—Profiles of the narrow component of Hβ (*a*) and of [O III] λ4959 (*b*) at the nucleus of NGC 5548. The "curved baseline" to Hβ occasioned by the broad-line component has been subtracted off by fitting a second-order polynomial to it. The flux scale is indicated by the vertical bars, which represent 5.0×10^{-16} ergs cm^{-2} s^{-1} Å^{-1} in (*a*) and 2.0×10^{-15} ergs cm^{-2} s^{-1} Å^{-1} in (*b*). The range of velocities plotted is 2600 km s^{-1} in both diagrams.

Figures 6*a* and 6*b* tabulate the measured FWHMs and standard deviations $\{[\sum_\lambda F_\lambda(\lambda - \bar{\lambda})^2/\sum_\lambda F_\lambda]^{1/2}\}$ of [O III] λ5007 and Hβ, after deconvolution from the instrumental resolution and interpolation onto a rectangular grid. The ratio of the widths FWHM/standard deviation is, in general, smaller than the value of 2.35 appropriate to a Gaussian function, indicating that the lines have relatively more power in their wings than do Gaussians. To within the errors, which are estimated to be ±30 km s^{-1} for strong lines and ±50 km s^{-1} for weak ones, [O III] λ5007 and Hβ have similar widths at the nucleus, despite the profile difference. Elsewhere the greater width of [O III] is clearly apparent. For upper limits to the widths of spectrally unresolved lines, we have given the very conservative values of 100 and 80 km s^{-1} (FWHM and standard deviation, respectively). Some unresolved lines detected at high signal-to-noise ratio are likely to be considerably narrower than these limits would indicate.

An interesting feature of Figure 6*a* is the possible displacement of the broadest [O III] λ5007 profiles from the nucleus (peak of continuum light). The broadest [O III] lines (FWHM ≃ 500 km s^{-1}) are found 1″–3″ north and west of the nucleus. Because we did not obtain a spectrum with the slit center 1.″25 south of the nucleus, we can say nothing about the line widths here. However, the lines are still very broad (≳400 km s^{-1}) ≃ 2.″5 south of the nucleus, although the error in their widths is substantial, because the peak fluxes here are ≲10% of that at the nucleus.

c) Velocity Field, Systemic Velocity, and Mass

The heliocentric velocity fields of [O III] λ5007 and Hβ are given in numerical form in Figure 7*a* (mean velocity) and 7*b* (velocity of line peak). The velocities of Hα and [N II] λ6584 in the single long-slit spectrum in p.a. 144° are in excellent agreement with each other (to <15 km s^{-1}). They increase from 5080 ± 10 km s^{-1} (heliocentric) at the southeast end of the nebulosity (7″ from the nucleus in p.a. 101°) to 5233 ± 10 km s^{-1} at the northwest end (6.″5 from the nucleus in p.a. 11°). In

	...	...	...	<100	150	190	190					
	<100	<100	<100	<100	...	...	...					
		130	200	170	130	150	200	100		<100	...	...
		<100	<100	<100	150	<100	...	...		<100	<100	<100
	180	200	190	190	290	240	260		160	160		
	...	<100	<100	<100	150	<100	<100		...	...		
	140			370	450	520	500					
	...			...	130	...	...					
				170	390*	470	470	390	340	250	230	
				...	310*	470	...	...	...	...	...	
				300	400	480	380					
				<100	150	140	...					
			210	300	290	300						
			<100	<100	...	...						
			220	300	300	260	290	120	160			
			...	...	...	...	...	...	...			

FIG. 6a

	...	...	...	<80	110	80	80					
	<80	<80	<80	<80	...	...	...					
		<80	90	80	80	140	110	<80		<80	...	...
		<80	<80	<80	<80	<80	...	...		<80	<80	<80
...	<80	80	130	170	170	150	170		<80	<80		
<80	...	<80	<80	<80	80	110	130		...	...		
	<80			220	270	260	280					
	...			...	150	...	...					
				150	190*	260	280	200	170	90	100	
				...	180*	190	...	...	...	...	...	
				170	240	220	210					
				<80	110	140	...					
			130	160	170	200						
			<80	<80	...	...						
			90	160	210	190	200	190	80			
			...	...	...	...	...	...	...			

FIG. 6b

FIG. 6.—Widths of emission lines (in km s^{-1}) in NGC 5548. At each location, a pair of numbers is given, one above the other. The upper number refers to [O III] λ5007 and the lower to Hβ. North is up, and east is to the left. The nucleus (peak of continuum light) lies to the west of the point indicated by the asterisk and 0.57 of the distance to the adjacent point. The vertical displacement between adjacent rows is 1".25, except immediately to the south of the nucleus, where it is 2".5. The horizontal displacement between adjacent columns is 1".65. (*a*) Full width at half-maximum; (*b*) standard deviation.

the region where this spectrum overlaps the grids in Figure 7, the velocities of Hα and [N II] λ6584 agree with those of Hβ to <15 km s^{-1}. We restrict our attention to the Hβ and [O III] λ5007 lines, with their more complete spatial coverage, in the following analysis of the gaseous kinematics.

The velocity fields (Fig. 7) show high velocities to the north and northwest of the nucleus and low velocities to the south. In order to determine the systemic velocity of NGC 5548, "rotation curves" in six different position angles were derived from the various two-dimensional maps. After omitting points within 1".5 of the nucleus (the velocity of which is clearly affected by the activity, as discussed below), smooth curves were fitted to the data for both mean and peak velocities. The systemic velocity was then calculated in two ways for each line: (1) by averaging all measurements more than 1".5 from the nucleus and (2) by taking the average of the velocities of the six fitted curves at the position of the nucleus. The values obtained from these two methods agree to within 20 km s^{-1}, and any difference between [O III] and Hβ is marginal. The mean value of all estimates—5133 $\pm$ 20 km s^{-1}—was finally adopted. This number agrees well with the 5142 km s^{-1} found by Mirabel and Wilson (1984) from a single-dish 21 cm hydrogen line profile. The systemic velocity with respect to the center of the Local Group is 5186 km s^{-1} (correction from de Vaucouleurs, de Vaucouleurs, and Corwin 1976), and the distance of NGC 5548 is 69 Mpc.

As can be seen in Figure 7, the nuclear velocities of narrow Hβ and [O III] λ5007 are below systemic. The offset is more than 100 km s^{-1} for the mean velocities and is also apparent in the peak values.[4] NGC 5548 thus follows the trend noted by Heckman *et al.* (1981), Mirabel and Wilson (1984), Whittle (1985), and Wilson and Heckman (1985) for the velocities (centroid, mean, or C50 parameter) of the narrow nuclear lines in active galaxies to be blueshifted with respect to the systemic velocity. This blueshift of the nuclear gas in NGC 5548 is

[4] The large difference in the velocities of the peak of Hβ between the two spectra straddling the nucleus results from the double-peaked profile, the blueward peak being slightly stronger in the western spectrum and the redward peak higher on the eastern side.

			...	93	69	88	92					
			40	72	...	...	...					
		28	26	39	53	164	130	66		102	...	...
		26	40	69	61	136	...	...		141	125	209
...	32	6	−55	36	81	112	195		113	100		
37	...	12	24	55	82	111	212		...	...		
	−28			−37	−70	−36	21					
	...			...	30	...	...					
				−120	−121*	−141	−97	−66	59	119	74	
				...	−86*	−164	...	...	...	...	...	
			...	−98	−119	−54	−69					
			−23	−44	−76	−11	...					
			−125	−73	−111	−66	...	...				
			−15	−23	−13	−20	−27	−33				
			−112	−131	−102	−111	−156	−178	32			
			...	...	...	−88	...	...	...			

FIG. 7*a*

			...	87	86	90	74					
			79	84	...	...	...					
		50	13	77	74	108	108	18		76	...	
		...	...	...	71	82	...	...		165	123	
	15	32	17	4	81	131	101		71	45		
	...	8	24	50	81	118	152		...	...		
	−37			3	6	−34	82					
	...			...	105	...	...					
				−111	−94*	−80	−74	−59	49	174	87	
				...	−14*	−187	...	...	...	...	...	
				−76	−98	−55	−16					
				...	−11	−9	...					
			−124	−69	−25	−25		...				
			−13	−16	−10	...		−31				
			−123	−40	−45	−60	−41	−41	−21			
			...	...	...	...	...	...	...			

FIG. 7*b*

FIG. 7.—Recession velocities (in km s^{-1}) of emission lines in NGC 5548, after subtraction of the heliocentric systemic velocity of 5133 km s^{-1} (see text). The format is identical with that of Fig. 6, with the upper number of each pair referring to [O III] λ5007 and the lower to Hβ. (*a*) Mean velocity; (*b*) velocity of line peak.

related to a *spatial* shift (by 1".6 = 540 pc) of the nucleus from the kinematic center of the rotation curve. Were this the only asymmetry in the nuclear environment of NGC 5548, one might readily ascribe it to radial motions plus dust obscuration of the gas at the nucleus (cf. Heckman *et al.* 1981). We have already noted, however, that the [O III] λ5007 line appears broader some 1"–3" north and west of the nucleus than at the nucleus itself. In fact, the broadest lines may coincide with the kinematic center of the rotation curve. A precisely analogous situation is found in NGC 2110, and possible interpretations were discussed by Wilson and Baldwin (1985). One model they considered had the true continuum light peak coincident with the kinematic center, but partially covered by a dust lane, so that the observed light peak appears offset. We argued against this picture for NGC 2110, and it may be ruled out for NGC 5548, because in both cases the compact nuclear radio source is coincident with the observed optical nucleus. For NGC 5548, the astrometric agreement is to better than 0".4 (Clements 1981; Wilson and Ulvestad 1982), a much smaller number than the 1".6 shift observed. Perhaps the line widths are dominated by radial motions over the entire nuclear vicinity, but the rapid gradient of rotational velocity at the kinematic center provides an extra broadening when sampled with a slit of finite width. An interesting recent development is the finding by Dressler and Richstone (1988) of a separation between the kinematic center and the light peak in M31, on the basis of spectra of the stellar component. Stellar rotation curves and spatially dependent velocity dispersions for Seyfert galaxies would probably be the most useful new data in constraining explanations of the offsets observed in their gaseous kinematics.

After allowing for the blueshifted nuclear gas, the velocity fields of Figure 7 clearly resemble conventional rotation curves. The velocities of [O III] λ5007 and Hβ are in good agreement (for both mean and peak values) to the north of the nucleus, where both lines are narrow. To the south there seems to be a trend for [O III] to be blueshifted, typically by 50 km s^{-1} with respect to Hβ. This probable displacement may be connected with the line-profile differences, which are particularly noticeable in the southern part of the nebulosity. At least to the north of the nucleus, the rotation axis of the [O III] emitting gas lies in p.a. 81° ± 5°. This direction is almost perpendicular to the major axis—p.a. 162°—of the inner part of

the [O III] image (§ III*a*), suggesting that at least some of the extended [O III] emitting gas lies in an inclined, rotating, flattened system. The velocity field shows that the rotation curve flattens or turns over at a radius of $\sim 3''$ from the nucleus, where the observed rotation velocity is 100–150 km s^{-1}. The situation for Hβ, for which fewer velocity measurements are available, is much less certain. The rotation axis of the Hβ emitting gas lies in a similar direction to that of the [O III], but the high Hβ velocities in the northwest corner hint that the rotation axis position angle for Hβ may be different.

The mass interior to a radius of $5''$ ($=1.7$ kpc) can be estimated from the rotation curve. Adopting an observed rotation velocity of 135 km s^{-1} and a disk inclination (angle between plane of disk and plane of sky) of $\sim 35°$. the true circular velocity is $\simeq 240$ km s^{-1} and the mass (assumed to be spherically distributed) is $\simeq 2 \times 10^{10}\ M_\odot$. The inclination was obtained from the outer isophotes of the [O III] λ5007 image (Fig. 3*b*) and the assumption that the gas lies in an intrinsically circular, thin disk. Although a similar inclination is indicated by the isophotes of the stellar disk at larger radii (Fig. 2), the major axis of the nuclear bulge and the diffuse ring lie in p.a. $\simeq 130°$–$140°$ (Fig. 2), so it is not clear whether the [O III] gas lies in the same plane as the stellar disk. Given the uncertainty in the measured velocity and inclination, the error in the mass could be $\sim \pm 50\%$. Further, the mass estimate is a lower limit, since no correction for "pressure support" of the gas has been included.

d) Line Fluxes and Flux Ratios

The total flux densities in [O III] λ5007 and (narrow) Hβ were measured at each location and are tabulated in Figure 8*a*. Their ratio is given in Figure 8*b* for positions where both lines are detected with adequate signal-to-noise ratio. The high-excitation gas ([O III] λ5007/H$\beta \simeq 10$) near the nucleus is characteristic of Seyfert nuclei. The excitation of the gas at the nucleus with velocities corresponding to the two peaks in the Hβ profile (Fig. 5) is high, with [O III] λ5007/H$\beta = 9.4$ for both peaks. Between the peaks, this ratio is 11.0. However, in view of the quite different kinematical structures of [O III] and Hβ here, the two lines probably arise in different regions. The ratio [O III] λ5007/Hβ decreases away from the nucleus and is especially small ($\sim$0.6–4) to the north where both lines are narrow. While the numbers in Figure 8 are subject to substantial uncertainty, it is clear that the broad component of the emission-line gas is of high excitation, while the narrow component is of low excitation.

Figure 9 shows plots of the logarithms of the flux ratios [N II] λ6584/Hα and ([S II] λ6716 + λ6731)/Hα against position along the slit for the single long-slit spectrum (in p.a. 144°; cf. Fig. 1) which includes these lines. The origin of position in this diagram corresponds to $6''$ due east of the nucleus. At the southeast and northwest extremities of the nebulosity covered by this spectrum, log ([N II] λ6584/Hα) $\simeq 0.06 \pm 0.06$, and log [([S II] λ6716 + λ6731)/Hα] $\simeq 0.0 \pm 0.06$, both of which are con-

	...	...	...	6.1	11	7.7	4.1				
	1.3	1.9	5.0	2.9	...	...	...				
		2.3	4.4	7.4	11	13	9.8	1.7		1.2	...
		3.9	4.5	2.7	3.1	3.0	...	...		1.3	2.0
...	2.6	4.7	4.7	9.2	25	28	17		3.2	2.6	
2.4	...	5.1	2.0	3.3	5.4	6.6	4.4		...	...	
	5.0			60	260	210	84				
	...			...	33	...	...				
				120	1100*	1000	280	57	11	5.5	5.3
				...	130*	100	21	...	...	...	...
				93	180	110	59				
				...	17	13	...				
			11	18	35	20					
			2.3	3.0	5.6	...					
			4.9	13	25	26	18	8.3	4.1		
			...	...	...	...	...	...	...		

FIG. 8*a*

			2.1						
	0.6	1.0	2.7	3.5	4.3	...	...	...	1.0
	0.9	2.4	2.8	4.6	4.2	3.9			
				7.9					
				8.7*	10.0	11.5			
				10.0	8.5				
		4.8	6.0	6.3					

FIG. 8*b*

FIG. 8.—Spatial distribution of line fluxes and flux ratios in NGC 5548. The orientation, location of the nucleus, and vertical/horizontal separations of the rows/columns are as in Fig. 6. (*a*) Total fluxes of [O III] λ5007 (*upper number*) and Hβ (*lower number*) in units of 10^{-16} ergs cm^{-2} s^{-1} through a $1''.65 \times 1''.5$ aperture. (*b*) Flux ratio [O III] λ5007/Hβ.

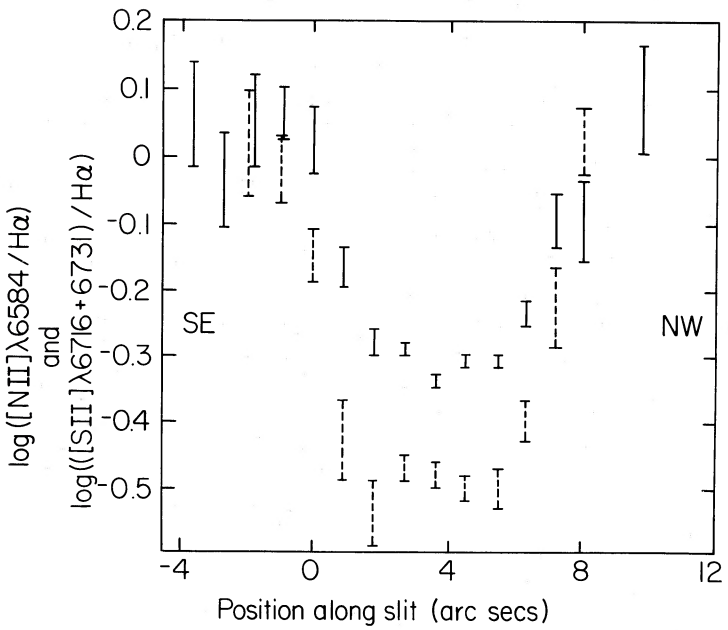

FIG. 9.–Plots of the logarithms of the flux ratios [N II] λ6584/Hα (*solid bars*) and ([S II] λ6716 + λ6731)/Hα (*dashed bars*) as a function of position along the slit, which was aligned in p.a. 144° and offset 6″ east of the nucleus (Fig. 1). This location 6″ due east of the nucleus was chosen as "position along slit = 0."

sistent with gas ionized by a power-law continuum spectrum or by shock waves, but higher than is appropriate to normal H II regions (Veilleux and Osterbrock 1987). In the nebulosity $\simeq 5''$ from the nucleus in p.a. 30°–50° (i.e., at position along slit $\simeq 2''$–$6''$ in Fig. 9), where [O III] λ5007/Hβ is low (Fig. 8*b*), log ([N II] λ6584/Hα) drops to -0.32 ± 0.04 and log [([S II] λ6716 + λ6731)/Hα] to -0.50 ± 0.02. Plots of log ([O III] λ5007/Hβ) against each of log ([N II] λ6584/Hα), log [([S II] λ6716 + λ6731)/Hα], and log ([O I] λ6300/Hα) at this location are given in Figure 10. Following Veilleux and Osterbrock (1987), the regimes occupied by normal H II regions, LINERs (shock-heated gas or gas photoionized by a very dilute power law; see Baldwin, Phillips, and Terlevich 1981; Halpern and Steiner 1983; Ferland and Netzer 1983), and power-law ionized gas are shown. In the first two diagrams (Figs. 10*a* and 10*b*) the nebulosity 5″ from the nucleus in p.a. 30°–50° lies right on the border between active galactic nuclei and H II region-like objects. However, the weakness of [O I] λ6300 here [log ([O I] λ6300/Hα) $= -1.47^{+0.15}_{-0.2}$] argues strongly against a significant contribution from LINER–type emission, for which log ([O I] λ6300/Hα) = −0.1 to −0.9. The low-excitation nebulosity to the northeast of the nucleus of NGC 5548 appears, therefore, to be dominated by H II regions, with some contribution from power-law ionized gas.

For this low-excitation gas, the ionized sulfur doublet ratio is $\lambda 6716/\lambda 6731 = 1.40 \pm 0.15$, in good agreement with the low-density limit, and implying $N_e < 800(T/10^4)^{1/2}$ cm^{-3}. The lines are weaker at the extremities of the nebulosity, so the density limit here is less strong, $N_e < 2500(T/10^4)^{1/2}$ cm^{-3}.

IV. DISCUSSION

a) The Composite Narrow-Line Region

The results of § III strongly suggest a composite nature for the extended "narrow" emission line gas[5] in NGC 5548. The broader component of this emission, which is seen in both Hβ and [O III] at the nucleus (Fig. 4), is clearly characteristic of active nuclei. The lines here are $\simeq 400$ km s^{-1} (FWHM; see Fig. 6*a*) wide, which is somewhat larger than the average for Seyfert galaxies (Whittle 1985; Wilson and Heckman 1985). The high excitation ([O III] λ5007/Hβ $\simeq 10$; see Fig. 8*b*) of the nuclear spectrum is also characteristic of conventional narrow-line regions. The [O III] lines are also broad *off* the nucleus and, at least to the south, the broad emission is of high excitation.

Hβ is always narrower than [O III] λ5007 (Fig. 6) and is especially narrow in the nebulosity several arcseconds to the northeast of the nucleus (Fig. 3, *top right*, and Fig. 4). Our measurements of the line ratio [O III] λ5007/Hβ cover the entire nebulosity and show that this ratio decreases away from the nucleus, and is especially small to the northeast, where Hβ is very narrow. Both the differing widths of Hβ and [O III] λ5007 and the large range (0.6–11.5) in their flux ratio imply the existence of at least two gaseous components. The nature of the low-excitation component cannot be defined unambiguously by the [O III] λ5007/Hβ ratio alone; both H II regions ionized by hot stars and LINER–type emission (gas ionized by shock waves or by a dilute power-law continuum) are consistent with this flux ratio. However, the additional measurements of [O I] λ6300, [N II] λλ6548, 6584, Hα, and [S II] λλ6717, 6731 in the nebulosity several arcseconds to the northeast of the nucleus strongly suggest that the low-excitation gaseous component there comprises H II regions ionized by hot stars. This northeast nebulosity appears to represent a mixture of power-law ionized gas and normal H II regions, the two components being projected on top of each other along the line of sight (Fig. 10). This finding does not rule out the possibility that some of the narrow-line, low-excitation emission elsewhere is LINER type; further measurements of line ratios over the rest of the nebulosity are required to check whether such a third component actually exists. The situation is, nevertheless, reminiscent of NGC 1068, for which Baldwin, Wilson, and Whittle (1987)

[5] We exclude from our discussion the *very* broad component of Hβ (broad-line region), which is, as expected, spatially unresolved in our data.

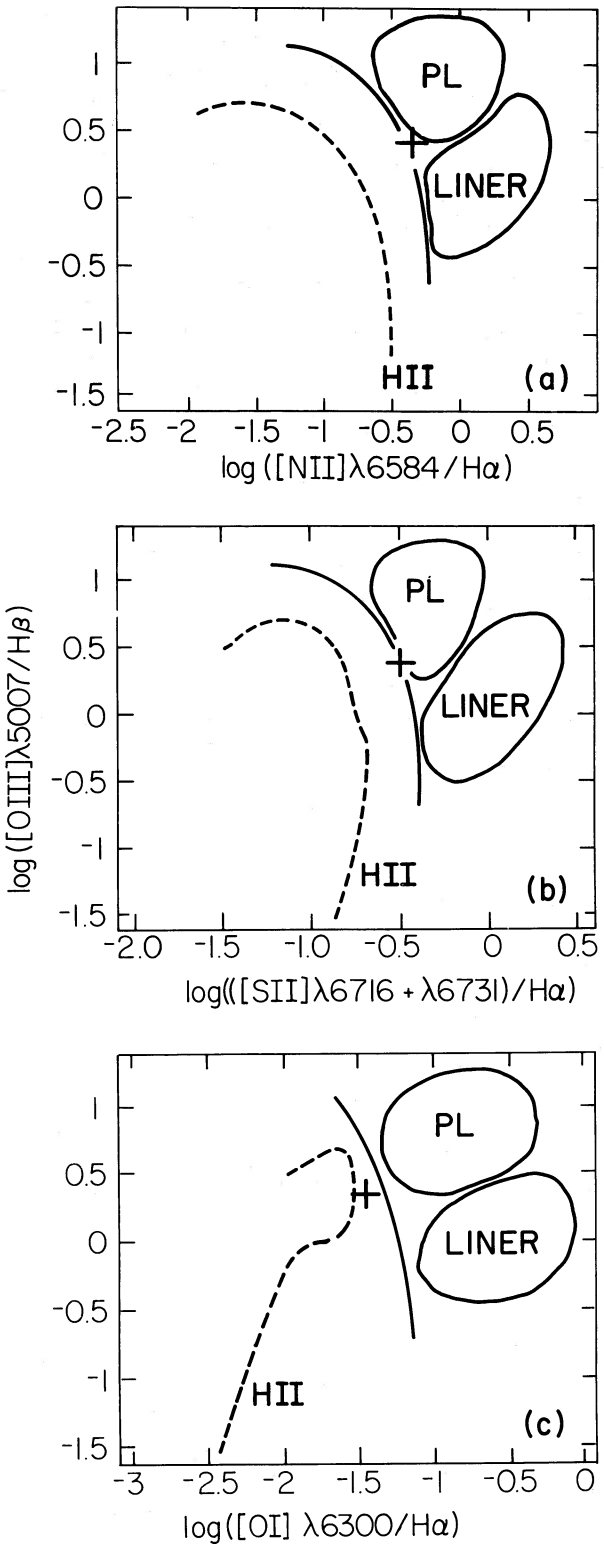

FIG. 10.—Plots of the logarithm of the flux ratio [O III] λ5007/Hβ against the logarithms of three other diagnostic line ratios: (*a*) [N II] λ6584/Hα, (*b*) ([S II] λ6716 + λ6731)/Hα, and (*c*) [O I] λ6300/Hα. Following Veilleux and Osterbrock (1987), the regimes occupied by power-law ionized gas (PL) and LINER–type emission are indicated. The solid curve separates active galactic nuclei from H II region–like objects, and the dashed curve represents H II region models of McCall, Rybski, and Shields (1985). The plus sign represents the low-excitation gas 5″ from the nucleus of NGC 5548 in p.a. 30°–50°.

plotted several diagrams involving emission-line ratios measured at many different locations in the disk of the galaxy. They found that the points in these diagrams fall in a band joining the regions occupied by power-law ionized gas and low-excitation H II regions. In NGC 1068, as in NGC 5548, [O III] λ5007 tends to be broader than Hβ. The Hβ emission from the northeast nebulosity in NGC 5548 is apparently dominated by H II regions, while the [O III] λ5007 emission at this location probably represents a mixture of the broad power-law ionized component and the narrow H II region component. Other galaxies for which optical spectroscopic investigations have shown composite Seyfert/H II nuclear properties include NGC 1365 (Phillips *et al.* 1983*a*), NGC 7469 (Wilson *et al.* 1986), NGC 7496 (Véron *et al.* 1981), NGC 7582 (Véron *et al.* 1981; Morris *et al.* 1985), IC 5135 and Mark 315 (Wilson and Baldwin 1988), and Mark 509 (Phillips *et al.* 1983*b*).

b) The High-Excitation Component

Our measurements of line width (Fig. 6) and flux ratio [O III] λ5007/Hβ (Fig. 8*b*) show that the [O III] λ5007 line is excited by the Seyfert nucleus in the bright inner parts of the nebulosity. As noted in § III*a*, these inner [O III] λ5007 isophotes (Fig. 3) are elongated in p.a. 162°, which is very close to the axis of the 13″ (4.4 kpc) size triple nuclear radio source (p.a. ≃ 160°; see Wilson and Ulvestad 1982). Such agreement between [O III] λ5007 and radio continuum axes is now known in about 15 Seyfert galaxies with "linear" radio sources (Haniff, Wilson, and Ward 1988). It is noteworthy that the [O III] isophotes in NGC 5548 are elongated in this sense on the 3″ scale, which is much closer to the nucleus than the outer radio lobes. This difference of scale argues against any direct role by the radio lobes themselves in the ionization of the thermal gas, but is consistent with the idea that the ionizing continuum is partially beamed along the radio axis (see Wilson, Ward, and Haniff 1988 and references therein). The data (Fig. 6) also suggest that the broadest [O III] lines are displaced from the continuum nucleus. This effect has been noticed in several other Seyferts with "linear" radio structures (e.g., NGC 5643; Morris *et al.* 1985; NGC 2110, Paper I; M51, Cecil 1988), and its origin is discussed briefly in § V.

In the outer parts of the [O III] λ5007 nebulosity, the major-axis position angle decreases to ≃140° (Fig. 3), which lies between the radio axis and the major axis of the nuclear bulge and inner ring/spiral arms (p.a. 125°–130°; Fig. 2). This suggests that some fraction of the outer [O III] emitting gas may lie in the disk of the galaxy. This would be in accord with the contribution of H II regions to the [O III] line on the north side of the nucleus beyond the bright inner region (§ IV*a*) and the apparent dominance of the velocity field here by rotational motions (§ III*c*).

c) The Low-Excitation Component

A complete analysis of the probable circumnuclear H II regions in NGC 5548 must await more extensive optical and infrared observations. In this subsection, we use the observed emission-line luminosity to estimate the number of hot stars present, argue that dust heated by these hot stars contributes negligibly to the mid- and far-infrared emission of NGC 5548, and show that insignificant radio emission results from the supernova remnants generated.

The long-slit data fully cover the nebulosity seen in the direct images and may be used to derive the total emission-line

luminosities, giving $F([\text{O III}]\ \lambda5007) \simeq 4.0 \times 10^{-13}$ ergs cm^{-2} s^{-1} and $F_{\text{total narrow}}(\text{H}\beta) \simeq 3.8 \times 10^{-14}$ ergs cm^{-2} s^{-1}. These numbers should be treated as lower limits, since faint emission may have been missed. Our value for $F([\text{O III}]\ \lambda5007)$ agrees well with that of 4.1×10^{-13} ergs cm^{-2} s^{-1} obtained by Ulvestad and Wilson (1982) through a 4".2 diameter aperture, but is smaller than 6.3×10^{-13} and 7.1×10^{-13} ergs cm^{-2} s^{-1}, the values found by Adams and Weedman (1975) and Anderson (1970) through 7".5–15" and 8" diameter apertures, respectively. The above-quoted value for $F_{\text{total narrow}}(\text{H}\beta)$ represents the sum of the high- and low-excitation components. A lower limit to the flux from the H II regions is $F_{\text{H II}}(\text{H}\beta) \approx 3 \times 10^{-15}$ ergs cm^{-2} s^{-1}, where only emission from the low-excitation nebulosity to the northeast of the nucleus, and more than 3" from it, has been included. If H II regions contribute to the rest of Hβ, this number will be too low. For example, including all Hβ emission except that from within 1".5 of the nucleus (where the line is clearly "contaminated" by the Seyfert nucleus), we find $F_{\text{H II}}(\text{H}\beta) \approx 9 \times 10^{-15}$ ergs cm^{-2} s^{-1}. In the following, $F_{\text{H II}} \approx 6 \times 10^{-15}$ ergs cm^{-2} s^{-1} is adopted, with recognition of its large uncertainty. The reddening of the H II regions is not known. Little obscuration is expected from our own Galaxy in view of the high Galactic latitude ($b = 70°.5$). If the *broad*-line region Balmer decrement [$F_B(\text{H}\alpha)/F_B(\text{H}\beta) = 4.21$; Osterbrock 1977] is treated as intrinsically case B, the absorption is $A_v \simeq 1.1$ mag. This value should represent an upper limit under more realistic conditions, in which the Balmer decrement is expected to be steeper than case B. Applying no reddening correction, the Hβ luminosity of the H II regions is $L_{\text{H II}}(\text{H}\beta) = 3.4 \times 10^{39}$ ergs s^{-1}. Under case B conditions, the ratio of ionizing photons to Hβ photons emitted following recombination is 8.5 (e.g., Osterbrock 1974), so the required number of ionizing photons for the H II regions is 7.0×10^{51} photons s^{-1}. For the starburst models calculated by Gehrz, Sramek, and Weedman (1983), the ratio $L(\text{bol})/L(\text{H}\alpha)$ ranges between 30 and 760, depending on the form of the initial mass function (see their Table 6). The bolometric luminosity of the circumnuclear hot stars in NGC 5548 is then expected to be $L(\text{bol}) \simeq 7.4 \times 10^7$–$1.9 \times 10^9\ L_\odot$. For the reasons summarized by Wilson *et al.* (1986), these numbers represent lower limits. The total infrared luminosity observed from NGC 5548 between 1 and 100 μm is $4.9 \times 10^{10}\ L_\odot$. This number was obtained from the near-infrared photometry by Rieke (1978) and the *IRAS* fluxes (Joint *IRAS* Science Working Group 1985); no correction has been applied for the differing resolutions of the near and far-infrared observations. Thus the massive stars inferred from the Hβ observations of the circumnuclear H II regions appear to be insignificant contributors to the bolometric luminosity. This conclusion is supported by the shape of the *IRAS* spectrum. With $\alpha(60, 25) = -0.34$ and $\alpha(100, 60) = -0.92$ ($S \propto \nu^\alpha$), the spectrum of NGC 5548 resembles those of quasars rather than nuclear starbursts or galaxy disks (cf. Miley, Neugebauer, and Soifer 1985). Although dust heated by hot stars could, in principle, contribute to the infrared emission if significant obscuration is present, it is probable that the mid- and far-infrared emission is dominated by the Seyfert nucleus.

The triple nuclear radio source of NGC 5548 (Wilson and Ulvestad 1982) is morphologically quite different from the Hα + [N II] image (Fig. 3). Thus radio emission generated by supernovae and supernova remnants resulting from the hot stars appears negligible. From Figure 1*b* of Wilson and Ulvestad (1982), an upper limit of <3.5 mJy may be obtained for the 1.4 GHz flux density of the prominent H II regions which lie in the northeast quadrant (Fig. 3) and are more than 1".4 east of the nucleus (the latter displacement excludes confusion by radio emission from the nucleus itself and the northern radio lobe). To confirm that insignificant radio emission would be expected in a "starburst" model, we note that the mean ratio of the supernova rate to the total luminosity is 2.9×10^{-12} (yr $L_\odot$)$^{-1}$ for the models computed by Rieke *et al.* (1980). Scaling to the luminosity range derived above for the hot stars in NGC 5548, one obtains a rate of 2.1×10^{-4} to 5.5×10^{-3} supernovae yr^{-1}. Ulvestad (1982) has estimated the expected radio emission for a given supernova rate assuming that the remnants obey the empirically determined Σ–D relation (e.g., Caswell and Lerche 1979) and are in the adiabatic phase. His equation (7) predicts a total flux density from the supernova remnants in NGC 5548 of $S(1.4\ \text{GHz}) = 0.002$–$0.07$ mJy, if the blast wave energy per remnant is 10^{50} ergs, the density of the ambient medium is 1 cm^{-3}, and the spectral index is 0.75. This range of flux density is consistent with the observational upper limit for the H II regions and is entirely negligible in comparison with the total flux density of the triple radio source, $S(1.4\ \text{GHz}) = 23$ mJy.

V. CONCLUSIONS

We have found that NGC 5548 contains a spatially extended, high-excitation, narrow-line region, with line widths ranging between 500 and 100 km s^{-1} (FWHM). This nebulosity is elongated along the axis of the triple radio source. The peak of optical continuum light (nucleus) coincides with the peak of the [O III] $\lambda5007$ distribution. However, the kinematic center of the rotation curve is displaced by 1".6 (= 540 pc) from this position, and the velocity of the nucleus is blueshifted by $\simeq 100$ km s^{-1} with respect to systemic. The broadest [O III] $\lambda5007$ lines may also be displaced from the nucleus, and their location is consistent with that of the kinematic center. These shifts are unlikely to result from partial obscuration of the true continuum nucleus by dust, because of the excellent agreement between the astrometric locations of the radio and optical nuclei. Similar shifts have been found in the gaseous kinematics of other active galaxies (e.g., NGC 2110, Wilson and Baldwin 1985; NGC 3310, van der Kruit 1976, Balick and Heckman 1982; NGC 4151, Heckman *et al.* 1981; and IC 5063 Bergeron, Durrett, and Boksenberg 1983). In NGC 2110 and NGC 5548, the velocity of the nucleus is not inconsistent with that of the rotation curve at its location, suggesting a real physical displacement between the nucleus and the mass center of the galaxy. However, in all cases where such a displacement between the nucleus and the kinematical center is seen, the nucleus is *blueshifted* with respect to systemic. Such a preferential blueshift is difficult to understand if the nucleus is following normal rotational motion, so it seems more likely that high-velocity radial motions of the nuclear ionized gas are responsible for the effect. Our finding that the broadest [O III] lines may be located in the vicinity of the kinematic center in NGC 5548 may result from the additional component of line broadening occasioned by sampling a rapid gradient of rotational velocity with a slit of finite width. Alternatively, the effect could be related to gaseous outflow in the bipolar flow which fuels the radio lobes.

In addition to the high-excitation gas, an extended, low-excitation component with narrow (FWHM < 100 km s^{-1}) lines is seen. The kinematics of this nebulosity are dominated by rotational motions, and the line ratios suggest that it is

ionized by hot stars, at least in the region to the northeast of the nucleus, and more than 3″ from it. The narrow, low-excitation component elsewhere may also originate in H II regions, but we have insufficient data on the line ratios to prove this; an alternative origin would involve LINER–type emission from gas ionized by shock waves or by the dilute nuclear continuum source. Under close scrutiny, an increasing number of Seyfert galaxies are being found to contain active star-forming regions in the environment of their nuclei, supporting suggestions that the two phenomena are related. Unlike NGC 1068 and NGC 7469, which contain starbursts of luminosity in excess of 10^{11} $L_{\odot}$, the luminosity of the stars needed to ionize the circumnuclear H II regions in NGC 5548 is quite modest, being of order 10^{8}–10^{9} $L_{\odot}$. For this reason our data cannot be taken to indicate a causal relation between star formation and the Seyfert activity in NGC 5548.

Our results may be of use to those investigating the variability of the broad lines in NGC 5548, because it is common practice to normalize the fluxes of [O III] $\lambda\lambda$4959, 5007 to the same value in the various spectra before intercomparing the profiles and fluxes of the broad lines. Since we find [O III] λ5007 to be extended by $\simeq$12″, this procedure is subject to some uncertainty as a result of fluctuations in seeing and telescope tracking. Our maps of this line should allow an estimate of the magnitude of this uncertainty in any particular set of observations of NGC 5548.

This research was supported by the National Science Foundation under grants AST 87-19207, AST 87-18363, and AST 86-12228 to the University of Maryland, Ohio State University, and the University of Washington, respectively, and through its funding of the National Optical Astronomy Observatories. We also thank NATO for grant 675/83 and the Computer Science Center of the University of Maryland for computer time. Support was also provided by the Graduate School Research Fund of the University of Washington and by National Aeronautics and Space Administration grant NAG 8529. John Ohlmacher provided invaluable assistance with the long-slit data. Dr. A. G. de Bruyn kindly allowed us to reproduce his plate. Part of this work was done while A. S. W. was at the Institute for Astronomy, University of Hawaii.

REFERENCES

Adams, T. F. 1977, *Ap. J. Suppl.*, **33**, 19.
Adams, T. F., and Weedman, D. W. 1975, *Ap. J.*, **199**, 19.
Anderson, K. S. 1970, *Ap. J.*, **162**, 743.
———. 1971, *Ap. J.*, **169**, 449.
Baldwin, J. A., Phillips, M. M., and Terlevich, R. 1981, *Pub. A.S.P.*, **93**, 5.
Baldwin, J. A., Wilson, A. S., and Whittle, M. 1987, *Ap. J.*, **319**, 84.
Balick, B., and Heckman, T. M. 1981, *Astr. Ap.*, **96**, 271.
Barr, P., Willis, A. J., and Wilson, R. 1983, *M.N.R.A.S.*, **203**, 201.
Bergeron, J., Durret, F., and Boksenberg, A. 1983, *Astr. Ap.*, **127**, 322.
Burbidge, G. R. 1970, *Ann. Rev. Astr. Ap.*, **8**, 369.
Caswell, J. L., and Lerche, I. 1979, *M.N.R.A.S.*, **187**, 201.
Cecil, G. 1988, *Ap. J.*, **329**, 38.
Chuvaev, K. K. 1987, in *IAU Symposium 121, Observational Evidence of Activity in Galaxies*, ed. E. Ye. Khachikian, K. J. Fricke, and J. Melnick (Dordrecht: Reidel), p. 203.
Clements, E. D. 1981, *M.N.R.A.S.*, **197**, 829.
Crenshaw, D. M., and Peterson, B. M. 1986, *Pub. A.S.P.*, **98**, 185.
de Bruyn, A. G. 1980, *Highlights Astr.*, **5**, 631.
de Bruyn, A. G., and Sargent, W. L. W. 1978, *A.J.*, **83**, 1257.
de Robertis, M. M. 1985, *Ap. J.*, **289**, 67.
de Vaucouleurs, G., de Vaucouleurs, A., and Corwin, H. 1976, *Second Reference Catalogue of Bright Galaxies* (Austin: University of Texas Press).
Dressler, A., and Richstone, D. O. 1988, *Ap. J.*, **324**, 701.
Elvis, M., Maccacaro, T., Wilson, A. S., Ward, M. J., Penston, M. V., Fosbury, R. A. E., and Perola, G. C. 1978, *M.N.R.A.S.*, **183**, 129.
Ferland, G. J., and Netzer, H. 1983, *Ap. J.*, **264**, 105.
Gehrz, R. D., Sramek, R. A., and Weedman, D. W. 1983, *Ap. J.*, **267**, 551.
Halpern, J. P., and Steiner, J. E. 1983, *Ap. J. (Letters)*, **269**, L37.
Haniff, C. A., Wilson, A. S., and Ward, M. J. 1988, *Ap. J.*, **334**, 104.
Hayes, M. J. C., Culhane, J. L., Blissett, R. J., Barr, P., and Bell Burnell, S. J. 1980, *M.N.R.A.S.*, **193**, 15P.
Heckman, T. M., Miley, G. K., van Breugel, W. J. M., and Butcher, H. R. 1981, *Ap. J.*, **247**, 403.
Joint *IRAS* Science Working Group. 1985, *Cataloged Galaxies and Quasars Observed in the IRAS Survey* (Pasadena: JPL).
Malkan, M. A., and Filippenko, A. V. 1983, *Ap. J.*, **275**, 477.
McAlary, C. W., McLaren, R. A., and Crabtree, D. R. 1979, *Ap. J.*, **234**, 471.
McCall, M. L., Rybski, P. M., and Shields, G. A. 1985, *Ap. J. Suppl.*, **57**, 1.
Miley, G. K., Neugebauer, G., and Soifer, B. T. 1985, *Ap. J. (Letters)*, **293**, L11.
Mirabel, I. F., and Wilson, A. S. 1984, *Ap. J.*, **277**, 92.
Morris, S. L., Ward, M. J., Whittle, M., Wilson, A. S., and Taylor, K. 1985, *M.N.R.A.S.*, **216**, 193.
Mushotzky, R. F., Marshall, F. E., Boldt, E. A., Holt, S. S., and Serlemitsos, P. 1980, *Ap. J.*, **235**, 377.
Osterbrock, D. E. 1974, *Astrophysics of Gaseous Nebulae* (San Francisco: Freeman).
———. 1977, *Ap. J.*, **215**, 733.
———. 1984, *Quart. J.R.A.S.*, **25**, 1.
Peterson, B. M. 1987, *Ap. J.*, **312**, 79.
Peterson, B. M., Foltz, C. B., Byard, P. L., and Wagner, R. M. 1982, *Ap. J. Suppl.*, **49**, 469.
Peterson, B. M., Korista, K. T., and Cota, S. A. 1987, *Ap. J. (Letters)*, **312**, L1.
Phillips, M. M., Baldwin, J. A., Atwood, B., and Carswell, R. F. 1983*b*, *Ap. J.*, **274**, 558.
Phillips, M. M., Turtle, A. J., Edmunds, M. G., and Pagel, B. E. J. 1983*a*, *M.N.R.A.S.*, **203**, 759.
Rieke, G. H. 1978, *Ap. J.*, **226**, 550.
Rieke, G. H., Lebofsky, M. J., Thompson, R. I., Low, F. J., and Tokunaga, A. T. 1980, *Ap. J.*, **238**, 24.
Simkin, S. M., Su, H. J., and Schwarz, M. P. 1980, *Ap. J.*, **237**, 404.
Stirpe, G. M., de Bruyn, A. G., and van Groningen, E. 1987, *Astr. Ap.*, **200**, 9.
Su, H. J., and Simkin, S. M. 1980, *Ap. J. (Letters)*, **238**, L1.
Tananbaum, H., Peters, G., Forman, W., Giacconi, R., and Jones, C. 1979, *Ap. J.*, **223**, 74.
Ulrich, M. H., and Boisson, C. 1983, *Ap. J.*, **267**, 515.
Ulvestad, J. S. 1982, *Ap. J.*, **259**, 96.
van der Kruit, P. C. 1976, *Astr. Ap.*, **49**, 161.
Veilleux, S., and Osterbrock, D. E. 1987, *Ap. J. Suppl.*, **63**, 295.
Véron, P., Véron, M. P., Bergeron, J., and Zuiderwijk, E. J. 1981, *Astr. Ap.*, **97**, 71.
Wamsteker, W., *et al.* 1984, in *Future of Ultraviolet Astronomy Based on Six Years of IUE Research* (NASA CP-2349), p. 148.
Ward, M. J., Elvis, M., Fabbiano, G., Carleton, N. P., Willner, S. P., and Lawrence, A. 1987, *Ap. J.*, **315**, 74.
Whittle, M. 1985, *M.N.R.A.S.*, **213**, 1.
Wilson, A. S., and Baldwin, J. A. 1985, *Ap. J.*, **289**, 124.
———. 1988, *A.J.*, submitted.
Wilson, A. S., Baldwin, J. A., Sun, S., and Wright, A. E. 1986, *Ap. J.*, **310**, 121.
Wilson, A. S., Baldwin, J. A., and Ulvestad, J. S. 1985, *Ap. J.*, **291**, 627 (Paper I).
Wilson, A. S., and Heckman, T. M. 1985, in *Proc. Seventh Santa Cruz Workshop on Astronomy and Astrophysics, Astrophysics of Active Galaxies and Quasi-stellar Objects*, ed. J. S. Miller (Mill Valley: University Science Books), p. 39.
Wilson, A. S., and Ulvestad, J. S. 1982, *Ap. J.*, **260**, 56.
Wilson, A. S., Ward, M. J., and Haniff, C. A. 1988, *Ap. J.*, **334**, 121.

J. A. BALDWIN: Department of Astronomy, Ohio State University, 174 West 18th Avenue, Columbus, OH 43210

B. BALICK: Astronomy Department, FM-20, University of Washington, Seattle, WA 98195

T. M. HECKMAN and A. S. WILSON: Astronomy Program, University of Maryland, College Park, MD 20742

XUENING, WU: 7 Chauncy Street, Cambridge, MA 02138